

VIBRATION AND BUCKLING OF ORTHOTROPIC SKEW PLATES

By S. DURVASULA, P. S. NAIR AND M. S. S. PRABHU

(Department of Aeronautical Engineering, Indian Institute of Science, Bangalore-12, India)

[Received : February 5, 1971]

ABSTRACT

In this paper the vibration and buckling problems of orthotropic skew plates with different edge conditions are formulated in a unified manner on the basis of orthotropic plate theory using the variational method of Ritz. A double series of beam characteristic functions appropriate to the particular combination of edge conditions is employed. The free vibration problem and the buckling problem of these orthotropic skew plates are then solved individually as particular cases of the general formulation. The orthotropic properties corresponding to grooved steel plate, fibre glass-epoxy and laminated boron-epoxy composite are used. Frequencies and nodal patterns of vibration as well as buckling coefficients under direct and shear loadings are obtained for rhombic plates with all edges clamped and also for plates with one pair of opposite edges clamped and the other pair simply supported. Comparison with available results is made where possible. In the case of the vibration problem, interesting features such as the crossing of frequency curves as observed in our earlier investigations on isotropic skew plates are observed in the case of orthotropic skew plates also. The symmetries of the nodal patterns and their variation with skew angle are also very interesting.

1. INTRODUCTION

The need for using orthotropic plate theory arises in the analysis of bending, buckling and vibration of wing panels either because of the anisotropy introduced in the manufacturing processes such as cold rolling or stretching of the metallic sheet or the use of stiffened construction, or more importantly, the use of modern fibre-reinforced composite materials. It is well known that the fibre-reinforced construction is being widely used in the design of aircraft and space vehicles. With the fabrication of composite laminates, the designer can now control the directional properties of these to a great extent thus resulting in an efficient design with better utilisation of

the material and achieve high strength/weight ratio. In recent years many such materials (Refs. 1, 2, 3) have been developed and are being extensively used.

For the calculation of dynamic response under deterministic or random excitation as also for an understanding of the panel flutter behaviour of plates, unstressed and stressed, of composite construction, a study of their vibration characteristics is essential. Equally, buckling strength characteristics of plates of composite construction used in these applications as well as in other engineering construction are important. Such plates can often be analysed using orthotropic plate theories. Investigations in this direction for the vibration characteristics of orthotropic rectangular plates with different material properties have been made by various authors⁴⁻⁹. Ashton and Anderson⁹, for example, studied both experimentally and theoretically the vibration characteristics of square laminated boron-epoxy composite plates with all edges clamped. The problems of buckling of orthotropic rectangular plates with opposite sides simply supported and having different boundary conditions on the other two sides are well covered in the literature¹⁰⁻¹³. The buckling coefficients of such plates can be deduced from the results of isotropic case^{14,15} and also from the corresponding frequency parameters of the orthotropic plate^{16,17}. The problem of generally orthotropic plates has also been studied in recent years^{18,19}. Ashton and Love²⁰ have carried out a series of experiments on rectangular boron-epoxy composite plates to determine the critical buckling loads. Ashton²¹ appears to have investigated this problem analytically also.

However, plates of other shapes such as parallelograms and trapeziums do not seem to have received much attention. Skew plates have obvious application in the construction of modern high speed aircraft and missiles with swept wings and tails. Evaluation of frequency parameters of vibration^{22,23} and buckling²⁴ coefficients of a few such plates were attempted by the authors in Refs. 22-24.

In this paper, we consider the problems of vibration and buckling of orthotropic skew plates with different edge conditions. The problem is formulated in oblique coordinates using the variational method of Ritz. Frequency parameters and buckling coefficients are presented for different skew angles for three representative material properties. The modes of vibration are plotted for one significant orthotropic property. Several interesting features concerning frequency curves and nodal patterns are observed.

Notation :

a, b	..	dimensions of the plate
A	..	matrix appearing in Eq. [19].
B	..	matrix appearing in Eq. [18].
C_{rs}	..	coefficient in the series expansion of deflection
D_{x_1}	..	$= E_{x_1} h^3 / 12 (1 - \nu_{x_1 y_1} \nu_{y_1 x_1})$
D_{y_1}	..	$= E_{y_1} h^3 / 12 (1 - \nu_{x_1 y_1} \nu_{y_1 x_1})$
$D_{x_1 y_1}$..	$= G_{x_1 y_1} h^3 / 12$
D_1	..	$= D_{y_1} \nu_{x_1 y_1} = D_{x_1} \nu_{y_1 x_1}$
E_{x_1}, E_{y_1}	..	Young's moduli of orthotropic material
E, F	..	matrices appearing in Eq. [15]
$G_{x_1 y_1}$..	shear modulus of orthotropic material
$H^{(1)}, H^{(2)}, H^{(3)}$..	matrices defined in Eq. [15]
h	..	plate thickness
I_{mr}^{pq}, J_{ns}^{pq}	..	integrals defined in Eq. [17]
$k^* a^2$..	frequency parameter, $\rho h \omega^2 a^4 / D_{y_1}$
k^2	..	$\rho h \omega^2 a^4 / \pi^4 D_{y_1}$
K	..	order of the matrix
M	..	maximum value of indices m, r
N	..	maximum value of indices n, s
N_x, N_y, N_{xy}	..	mid-plane forces (oblique components) $h \sigma_x, h \sigma_y, h \sigma_{xy}$ respectively
$N_{x_1}, N_{y_1}, N_{x_1 y_1}$..	mid-plane forces (orthogonal components) $h \sigma_{x_1}, h \sigma_{y_1}, h \sigma_{x_1 y_1}$ respectively
m, n, r, s	..	integers
M_n	..	normal bending moment
$\bar{R}_x, \bar{R}_y, \bar{R}_{xy}$..	non-dimensional mid-plane force parameters; $\sigma_x b^2 h / \pi^2 D_{y_1}, \sigma_y b^2 h / \pi^2 D_{y_1}, \sigma_{xy} b^2 h / \pi^2 D_{y_1}$ respectively
$\bar{R}_x^*, \bar{R}_y^*, \bar{R}_{xy}^*$..	non-dimensional mid-plane force parameters, $\sigma_x a^2 h \cos \psi / \pi^2 D_{y_1}, \sigma_y a^2 h \cos \psi / \pi^2 D_{y_1},$ $\sigma_{xy} a^2 h \cos \psi / \pi^2 D_{y_1}$ respectively

S	. . . domain of the plate
T	. . . maximum kinetic energy
U	. . . total potential energy of the plate
$w(x, y, t)$. . . time dependent plate deflection
$W(\xi, \eta)$. . . deflection of the plate
$X_m(\xi), Y_n(\eta)$. . . beam characteristic functions
x_1, y_1, z_1	. . . orthogonal coordinate system defined in Fig. 1
x, y, z	. . . oblique coordinate system defined in Fig. 1
ξ, η	. . . non-dimensional coordinates, $x/a, y/b$ respectively.
$\nu_{x_1y_1}, \nu_{y_1x_1}$. . . Poisson's ratios of orthotropic material
ρ	. . . mass density of the plate material
α	. . . $= D_{x_1}/D_{y_1}$
γ	. . . $= D_1/D_{y_1}$
δ, δ_{mnr}	. . . $= D_{x_1y_1}/D_{y_1}$ and Kronecker delta respectively
$\sigma_x, \sigma_y, \sigma_{xy}$. . . oblique stress components defined in Fig. 1
∇_s^2	. . . skew differential operator $= \sec^2 \psi \left(\frac{\partial^2}{\partial x^2} - 2 \sin \psi \frac{\partial^2}{\partial x \partial y} + \frac{\partial^2}{\partial y^2} \right)$
ψ	. . . skew angle, as defined in Fig. 1
λ	. . . $= a/b$, side ratio
ϕ	. . . phase angle defined in Eq. [2]
ω	. . . circular frequency in radians/sec.

2. MATHEMATICAL FORMULATION

A sketch of the skew plate is shown in Fig. 1, along with the oblique stress system used in the analysis. The plate is assumed to be thin, uniform and orthotropic.

The boundaries of the plate in oblique coordinates are

$$x=0, \quad x=a; \quad y=0, \quad y=b \quad [1]$$

For a plate vibrating in its natural mode, the deflection can be expressed as

$$w(x, y, t) = W(x, y) \sin(\omega t + \phi) \quad [2]$$

where $W(x, y)$ is the mode shape of deflection.

Using the classical small deflection thin plate theory, the differential equation for the vibration of a plate of constant thickness under the action of middle surface forces is given by

$$D_{x_1} w, x_1 x_1 x_1 + 2 (D_1 + 2D_{x_1 y_1}) w, x_1 x_1 y_1 y_1 + D_{y_1} w, y_1 y_1 y_1 y_1 + N_{x_1} w, x_1 x_1 + 2 N_{x_1 y_1} w, x_1 y_1 + N_{y_1} w, y_1 y_1 + \rho h w, u = 0 \quad [3]$$

The boundary conditions considered are combinations of clamped and simply supported conditions. For a simply supported edge, the boundary conditions are

$$W = 0, M_n = 0 \quad [4]$$

For a polygonal boundary these can be written as

$$W = 0, \nabla_n^2 W = 0 \quad [5]$$

The boundary conditions for clamped edge are given by

$$W = 0, \partial W / \partial n = 0 \quad [6]$$

where n denotes the direction of the outward normal to the edge. It can be shown that the boundary condition $\partial W / \partial n = 0$ in Eq. [6] reduces to

$$\begin{aligned} \partial W / \partial x = 0 \text{ on } x = 0 \text{ and } a \\ \partial W / \partial y = 0 \text{ on } y = 0 \text{ and } b \end{aligned} \quad [7]$$

An approximate solution of the problem as stated by the Eq. [3], together with the boundary conditions such as given by Eqs. [4, 5, 6] as appropriate to each edge, is solved using the variational method of Ritz.

From the classical small deflection thin plate theory, the total potential energy of the vibrating plate in orthogonal coordinates is given by

$$\begin{aligned} U = \frac{1}{2} \iint_S (D_{x_1} W^2, x_1 x_1 + D_{y_1} W^2, y_1 y_1 + 2 D_1 W, y_1 y_1 W, x_1 x_1 \\ + 4 D_{x_1 y_1} W^2, x_1 y_1 - N_{x_1} W^2, x_1 - 2 N_{x_1 y_1} W, x_1 W, y_1 \\ - N_{y_1} W^2, y_1) dx_1 dy_1 \end{aligned} \quad [8]$$

The maximum kinetic energy is given by,

$$T = \frac{1}{2} \rho h \omega^2 \iint_S W^2 dx_1 dy_1 \quad [9]$$

Non-dimensional coordinates ξ and η are defined as follows .

$$\xi = x/a; \quad \eta = y/b \quad [10]$$

For the stress system shown in Fig. 1, the expressions for the total potential energy and maximum kinetic energy of the plate are given respectively by,

$$\begin{aligned}
 U = \int_0^1 \int_0^1 (b \cos \psi D_{y_1} / 2a^2) [& \{ \alpha W^2_{,\xi\xi} + (\tan^2 \psi W_{,\xi\xi} - 2 \lambda \tan \psi \sec \psi W_{,\xi\eta} \\
 & + \lambda^2 \sec^2 \psi W_{,\eta\eta})^2 + 2 \gamma W_{,\xi\xi} (\tan^2 \psi W_{,\xi\xi} - 2 \lambda \tan \psi \sec \psi W_{,\xi\eta} \\
 & + \lambda^2 \sec^2 \psi W_{,\eta\eta}) + 4 \delta (\lambda \sec \psi W_{,\xi\eta} - \tan \psi W_{,\xi\xi})^2 \} \\
 & - (b/2a) \{ N_x W_{,\xi}^2 + 2 \lambda N_{xy} W_{,\xi} W_{,\eta} + \lambda^2 N_y W_{,\eta}^2 \}] d\xi d\eta \quad [11]
 \end{aligned}$$

and

$$T = \frac{1}{2} \omega^2 ab \rho h \cos \psi \int_0^1 \int_0^1 W^2 d\xi d\eta \quad [12]$$

The mode shape W is expressed as a double series in terms of the "admissible functions", that is, functions which satisfy geometric boundary conditions. Beam characteristic functions which have been extensively used in the literature have been used in the present paper. $W(\xi, \eta)$ is expressed in terms of these functions as

$$W(\xi, \eta) = \sum_{m=1}^M \sum_{n=1}^N C_{mn} X_m(\xi) Y_n(\eta) \quad [13]$$

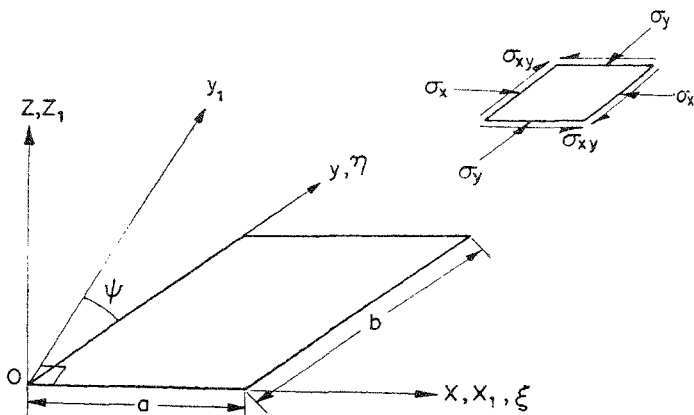


FIG. 1

Sketch of Skew Plate and the Oblique In-plane Stress System

where $X_m(\xi)$ and $Y_n(\eta)$ are the beam functions satisfying the boundary conditions considered.

The coefficients C_{mn} of the series are determined from the condition

$$\frac{\partial (U - T)}{\partial C_{mn}} = 0 \quad [14]$$

Using expressions for U and T in Eq. [14] a set of simultaneous homogeneous, linear, algebraic equations are obtained which can be expressed as

$$\sum_{r=1}^M \sum_{s=1}^N C_{rs} (\alpha B_{mnr s} + D_{mnr s} + \gamma E_{mnr s} + 4 \delta F_{mnr s} - \bar{R}_x^* H_{mnr s}^{(1)} - \bar{R}_y^* H_{mnr s}^{(2)} - \bar{R}_{xy}^* H_{mnr s}^{(3)} - k^* \delta_{mnr s}) = 0 \quad [15]$$

where

$$\begin{aligned} B_{mnr s} &= I_{mr}^{22} J_{ns}^{00} \\ D_{mnr s} &= \lambda^4 \sec^4 \psi I_{mr}^{00} J_{ns}^{22} - 2 \lambda^3 \sec^3 \psi \tan \psi (I_{mr}^{01} J_{ns}^{21} + I_{mr}^{10} J_{ns}^{12}) \\ &\quad + \lambda^2 \sec^2 \psi \tan^2 \psi (I_{mr}^{02} J_{ns}^{20} + 4 I_{mr}^{11} J_{ns}^{11} + I_{mr}^{20} J_{ns}^{02}) \\ &\quad - 2 \lambda \tan^3 \psi \sec \psi (I_{mr}^{12} J_{ns}^{10} + I_{mr}^{21} J_{ns}^{01}) + \tan^4 \psi I_{mr}^{22} J_{ns}^{00} \\ E_{mnr s} &= \lambda^2 \sec^2 \psi (I_{mr}^{02} J_{ns}^{20} + I_{mr}^{20} J_{ns}^{02}) - 2 \lambda \sec \psi \tan \psi (I_{mr}^{12} J_{ns}^{10} + I_{mr}^{21} J_{ns}^{01}) \\ &\quad + 2 \tan^2 \psi I_{mr}^{22} J_{ns}^{00} \\ F_{mnr s} &= \lambda^2 \sec^2 \psi I_{mr}^{11} J_{ns}^{11} - \lambda \tan \psi \sec \psi (I_{mr}^{12} J_{ns}^{10} + I_{mr}^{21} J_{ns}^{01}) + \tan^2 \psi I_{mr}^{22} J_{ns}^{00} \\ H_{mnr s}^{(1)} &= I_{mr}^{11} J_{ns}^{00}; \quad H_{mnr s}^{(2)} = \lambda^2 I_{mr}^{00} J_{ns}^{11}; \quad H_{mnr s}^{(3)} = 2 \lambda I_{mr}^{10} J_{ns}^{01} \end{aligned} \quad [16]$$

I_{mr}^{pq} , J_{ns}^{pq} are integrals of products of beam functions and their derivatives defined as follows:

$$I_{mr}^{pq} = \int_0^1 X_m^p(\xi) X_r^q(\xi) d\xi; \quad J_{ns}^{pq} = \int_0^1 Y_n^p(\eta) Y_s^q(\eta) d\eta \quad [17]$$

where p and q represent the order of the derivative and m, n and r, s are the mode numbers of the assumed beam functions. The formulae for the integrals were given in Ref. 25 and the numerical values of these integrals can be found in Ref. 26. Eq. [15] corresponding to orthotropic skew plates with different combinations of boundary conditions can be obtained by using integrals I_{mr}^{pq} , J_{ns}^{pq} appropriate to the particular end conditions, clamped, simply supported or free. However, in this paper, we consider skew plates either clamped allround or with a pair of opposite edges clamped and the other pair simply supported. Eq. [15] may be written in matrix form as

$$(\alpha[B] + [D] + \gamma[E] + 4\delta[F])\{C_{rs}\} = \bar{R}_x^* [H^{(1)}]\{C_{rs}\} + \bar{R}_y^* [H^{(2)}]\{C_{rs}\} \\ + \bar{R}_{xy}^* [H^{(3)}]\{C_{rs}\} + k^{*2}\{C_{rs}\} \quad [18]$$

Eq. [18] then represents the algebraic eigenvalue problem corresponding to vibration of stressed orthotropic skew plates. From this unified formulation the eigenvalue problem corresponding to the vibration problem of unstressed plates as well as the buckling problem with N_x , N_y or N_{xy} present individually or in combination, can be obtained by retaining the appropriate terms.

For example, the natural vibration problems of unstressed plate is given by

$$[A]\{C_{rs}\} = k^{*2}\{C_{rs}\} \quad [19]$$

where

$$[A] = \alpha[B] + [D] + \gamma[E] + 4\delta[F] \quad [20]$$

k^{*2} being the eigenvalue corresponding to frequency of vibration. On the other hand, the equation corresponding to the buckling problem under combined loading is given by

$$[A]\{C_{rs}\} = \bar{R}_x^* [H^{(1)}]\{C_{rs}\} + \bar{R}_y^* [H^{(2)}]\{C_{rs}\} + \bar{R}_{xy}^* [H^{(3)}]\{C_{rs}\} \quad [21]$$

The buckling problem is solved by assigning numerical values to any two of the three parameters \bar{R}_x^* , \bar{R}_{xy}^* , \bar{R}_y^* and treating the remaining one as the eigenvalue. For example, if the buckling parameter \bar{R}_x^* is to be obtained in the presence of N_y and N_{xy} , appropriate values are assigned to \bar{R}_y^* and \bar{R}_{xy}^* , and the equation is written as

$$[\bar{A}]^{-1} [H^{(1)}]\{C_{rs}\} = (1/\bar{R}_x^*)\{C_{rs}\} \quad [22]$$

where,

$$[\bar{A}] = \alpha[B] + [D] + \gamma[E] + 4\delta[F] - \bar{R}_y^* [H^{(2)}] - \bar{R}_{xy}^* [H^{(3)}] \quad [23]$$

Eq. [22] corresponds to the buckling problem with $1/\bar{R}_x^*$ as the eigenvalue. The eigenvalues k^{*2} and $1/\bar{R}_x^*$ of Eqs. [19] and [22] can be solved by any one of the standard methods.

For combinations of boundary conditions skew symmetric about the diagonals the two Eqs. [19] and [22] corresponding to the vibration and buckling problem respectively can be split into two cases: $(m+n)$ and $(r+s)$ Even; $(m+n)$ and $(r+s)$ Odd. The Even case corresponds to skew symmetric modes and the Odd case corresponds to skew antisymmetric modes. This

splitting reduces the order of the matrix whose eigenvalues and eigenvectors are to be determined. If $K (= M \times N)$ is the order of the original matrix, then the orders for the Even and Odd cases will be respectively $(K+1)/2$ and $(K-1)/2$ if K is Odd and $K/2$ if K is Even. For the buckling problem the lower of the two lowest eigenvalues obtained from the two cases is taken as the critical buckling load. For cases where symmetry of boundary conditions about the diagonals is not there, this splitting is not possible and the full matrix of order K will have to be handled both in the case of vibration and buckling problems.

In the case of the vibration problem, the eigenvector $C_{mn}^{(i)}$ is made use of for the calculation of the mode shape.

The entire plate is superimposed by l equispaced lines in the y -direction and k lines in the x -direction. The deflection at these grid points are calculated using Eq. [13] as follows :

$$W_{lk}^{(i)} = \sum_m^M \sum_n^N C_{mn}^{(i)} X_m(\xi_l) Y_n(\eta_k) \quad [24]$$

where l and k specify the point on the plate; i is the mode number; $X_m(\xi_l)$, $Y_n(\eta_k)$ values of X_m and Y_n at ξ_l and η_k respectively $C_{mn}^{(i)}$ is the i^{th} eigenvector from Eq. [19].

In matrix form Eq. [24] may be written as

$$[W_{lk}^{(i)}] = [A_{rslk}] \{C_{mn}^{(i)}\} \quad [25]$$

where

$W_{lk}^{(i)}$ = deflection of i^{th} mode at point (ξ_l, η_k)

$A_{rslk} = X_r(\xi_l) \times Y_s(\eta_k)$

$C_{mn}^{(i)}$ = i^{th} eigenvector

For symmetric combinations of boundary conditions the deflections of only one half of the plate, that is, the lower or upper triangle, need be considered. For other combinations of boundary conditions the whole plate is to be considered. Nodal patterns are then plotted from this mode shape information.

3. NUMERICAL CALCULATIONS

Vibration Problem: Numerical calculations for frequency parameter k^*2 have been made for rhombic plate for different skew angles with two combinations of boundary conditions, namely, all edges clamped (CCCC case) and one pair of opposite edges clamped and the other pair simply supported

(CSCS case). The orthotropic properties considered correspond to grooved steel plate, fibre glass-epoxy and laminated boron-epoxy composite. The number of terms was taken upto $M=N=6$ which results in matrices of order 18×18 each for the Even and Odd cases. The nodal patterns for different skew angles for the two combinations of boundary conditions are plotted from the mode shape data. For the rhombic CCCC and CSCS cases considered the deflections at 190 points (obtained by dividing the plate into 20 equal divisions in both x and y -directions) of the lower triangle of the plate are calculated for plotting these nodal patterns.

Buckling Problem: Buckling coefficients have been calculated for N_x and N_y each acting alone for all the cases considered for the vibration analysis. From the convergence study carried out for the buckling of isotropic case, it was decided to have terms upto $M=N=6$ for $\psi \leq 30^\circ$ and $M=N=8$ for $\psi > 30^\circ$.

4. RESULTS AND DISCUSSION

Vibration Problem: Numerical results for the first 6 frequencies of rhombic plates with $\psi=0^\circ, 15^\circ, 30^\circ$ and 45° are presented. The values are given in terms of the parameter k . A comparison of the present results for $\psi=0^\circ$ with those given by Ashton and Anderson is made in Table 1 and the agreement is satisfactory. Table 2 gives the first 6 frequencies of the CCCC plate for different orthotropic properties and skew angles. Numerical results are not available for comparison in the case of skew plates. Even in the case of rectangular plates (CSCS case) direct comparison has not been possible with the results of Ref. 17 for the reason that the orientation of the two principal axes of orthotropy is not the same relative to the clamped and simply supported edges.

In Table 3 the first 6 frequencies of the CSCS plates are given for the three different materials considered.

TABLE I

Clamped Square Plate, $a=12''$, $h=0.042''$, $\rho=0.192 \times 10^{-3}$ lb-sec²/in⁴
 $E_{x_1}=3.1 \times 10^7$ psi, $E_{y_1}=2.7 \times 10^6$ psi, $\nu_{x_1y_1}=0.28$, $G=0.75 \times 10^6$ psi
 $(\alpha=11.4815, \gamma=0.280, \delta=0.2759)$

Mode No.	1	2	3	4	5	6	7	8
Present Paper	128 ^a	163	238	338	354	360	409	496
Ashton and	125 ^b	159	238	329	350	343	397	482
Anderson (Ref. 9)	107 ^c	123	204	283	301	343	360	451

^a $M=6, N=6$, calculations; ^b $M=7, N=7$, calculations; ^c Experimental results

Note: Frequencies are given in Hz.

TABLE 2

Frequency parameters $k=(\rho h/D_{y1})^{1/2} a^2 \omega/\pi^2$ of composite rhombic plates (CCCC)

Material	ψ Mode	0°	15°	30°	45°
Grooved Steel Plate (Ref. 17) $\alpha = 1.265$, $\gamma = 0.28$ $\delta = 0.339$	1	3.814 (E)	4.031 (E)	4.819 (E)	6.800 (E)
	2	7.503 (0)	7.674 (0)	8.599 (0)	11.13 (0)
	3	8.077 (0)	8.77 (0)	10.98 (0)	15.7 (E)
	4	11.36 (E)	11.55 (E)	12.6 (E)	16.3 (0)
	5	13.4 (E)	14.4 (E)	17.3 (E)	21.0 (0)
	6	14.7 (E)	15.7 (E)	17.5 (0)	24.0 (E)
Glass-epoxy (Ref. 3) $\alpha = 2.963$, $\gamma = 0.25$ $\delta = 0.4532$	1	4.887 (E)	5.091 (E)	5.841 (E)	7.776 (E)
	2	8.210 (0)	8.606 (0)	9.951 (0)	12.92 (0)
	3	11.56 (0)	11.99 (0)	13.67 (0)	18.4 (E)
	4	13.9 (E)	13.96 (E)	15.2 (E)	18.6 (0)
	5	14.3 (E)	15.6 (E)	19.1 (E)	25.4 (0)
	6	19.3 (0)	19.0 (0)	21.0 (0)	26.8 (E)
Boron-epoxy (Ref. 9) $\alpha = 11.4815$, $\gamma = 0.28$ $\delta = 0.2759$	1	8.166 (E)	8.294 (E)	8.807 (E)	10.33 (E)
	2	10.37 (0)	10.77 (0)	12.23 (0)	15.87 (E)
	3	15.15 (E)	15.92 (E)	18.55 (E)	23.9 (0)
	4	21.5 (0)	21.7 (0)	22.52 (0)	25.3 (E)
	5	22.5 (0)	23.3 (E)	25.3 (E)	31.8 (E)
	6	22.9 (E)	23.5 (0)	26.6 (0)	33.0 (0)

TABLE 3

Frequency parameters $k=(\rho h/Dy_1)^{1/2} a^2 \omega/\pi^2$ of composite rhombic plate (CSCS)

Material	ψ MoJe	0°	15°	30°	45°
Grooved Steel Plate (Ref. 17), $\alpha = 1.265$ $\gamma = 0.28$, $\delta = 0.339$	1	3.142 (E)	3.318 (E)	3.969 (E)	5.64 (E)
	2	5.639 (0)	5.893 (0)	6.790 (0)	8.97 (0)
	3	7.701 (0)	8.187 (0)	10.00 (0)	13.4 (E)
	4	10.04 (E)	9.94 (E)	10.75 (E)	14.7 (0)
	5	10.4 (E)	11.6 (E)	14.5 (E)	18.0 (0)
	6	14.5 (0)	14.4 (0)	15.3 (0)	21.0 (E)
Glass-epoxy (Ref. 3) $\alpha = 2.963$, $\gamma = 0.25$ $\delta = 0.4532$	1	4.370 (E)	4.530 (E)	5.130 (E)	6.720 (E)
	2	6.525 (0)	6.833 (0)	7.902 (0)	10.37 (0)
	3	11.02 (E)	11.42 (E)	12.76 (E)	15.84 (E)
	4	11.29 (0)	11.7 (0)	13.2 (0)	17.3 (0)
	5	13.2 (E)	13.9 (E)	16.6 (E)	22.2 (0)
	6	17.1 (0)	17.1 (0)	18.4 (0)	23.1 (E)
Boron epoxy (Ref. 9) $\alpha = 11.4815$, $\gamma = 0.28$ $\delta = 0.2759$	1	7.879 (E)	7.966 (E)	8.33 (E)	9.46 (E)
	2	9.125 (0)	9.397 (0)	10.4 (0)	13.1 (0)
	3	12.59 (E)	13.18 (E)	15.3 (E)	19.9 (E)
	4	18.65 (0)	21.56 (0)	22.1 (0)	24.6 (0)
	5	21.38 (0)	22.6 (E)	22.8 (0)	28.6 (0)
	6	22.3 (E)	25.3 (0)	24.2 (E)	29.1 (E)

In Fig. 2 the frequency parameters of different modes of CCCC and CSCS plates are plotted against skew angle. The degeneracies observed in the case of square isotropic plate (Ref. 27) disappear now as a result of the asymmetries introduced by the material properties. The pattern of frequency crossings also is different as may be expected.

Fig. 2 (a) gives the variation of the frequencies of mildly orthotropic material (grooved steel plate) for the two boundary conditions considered. In CCCC case the frequency crossings are seen to be between the 3rd and the 4th at about 41° , between 5th and 7th at about 35° and between 6th and 7th at about 21° . In CSCS plate the 4th and 5th as well as the 6th and 7th frequencies are nearly degenerate pairs in the case of square geometry. The frequency crossings take place at about 37° between the 5th and 6th modes at about 40° between 3rd and 4th modes. Fig. 2 (b) is a plot of frequencies against skew angle for a particular fibre glass-epoxy composite plate. The only crossings observed among the first 6 modes for $\psi \leq 45^\circ$ are between 5th and 6th at about 40° in CCCC case and at about 41° in the CSCS case. The variation of frequencies of a strongly orthotropic material, namely, unidirectional boron-epoxy composite laminate is shown in Fig. 2(c). The frequency crossing are now seen to be between 5th and 6th at about 10° and between 7th and 8th at about 42° in plates with clamped boundaries. The manner of variation of frequencies for boron-epoxy plate with CSCS boundary condition appears to be rather different for higher frequencies for the configurations considered. This may be attributed to the unidirectional and hence highly anisotropic nature of the material as also the fact that the edges $x=0$, $x=a$ are clamped while the edges $y=0$, $y=b$ are only simply supported. In this case (CSCS), the frequency crossings are seen to be between the 5th and 6th modes at about 3° and also at 24° and between the 4th and 5th at about 28° .

Fig. 3-6 gives the nodal patterns corresponding to the frequencies in Table 2 for boron-epoxy composite. It may be seen that due to the orientation of all the plies of the laminated plate in the x -direction more number of nodal lines appear across the y -axis even in the CCCC plate. This is even more so in the case of CSCS case (Fig. 7-10) as the edges $y=0$ and $y=b$ are simply supported. Results of nodal patterns for other material properties are not plotted.

Buckling Problem: In Table 4, the buckling coefficients \bar{R}_x and \bar{R}_{xy} are given for two different boundary conditions, namely, CCCC and CSCS under both N_x and N_{xy} , each acting alone, for different skew angles 0° , 15° , 30° and 45° for a grooved steel plate. In Tables 5 and 6, the results for the above mentioned combinations of boundary conditions, loading and skew angle are given for fibre glass-epoxy respectively.

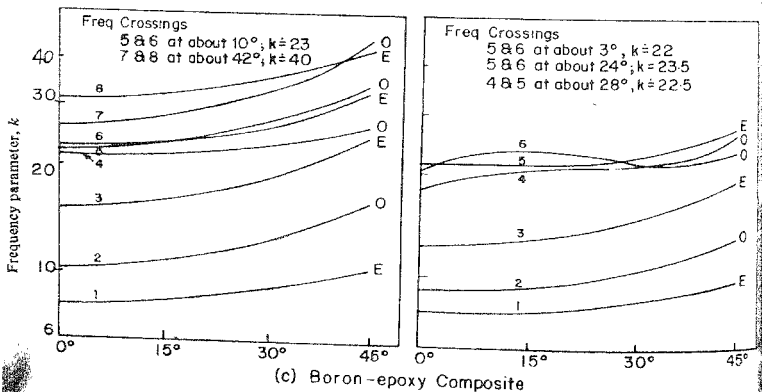
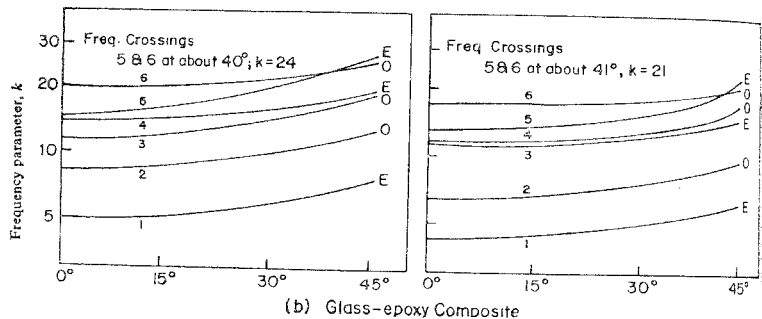
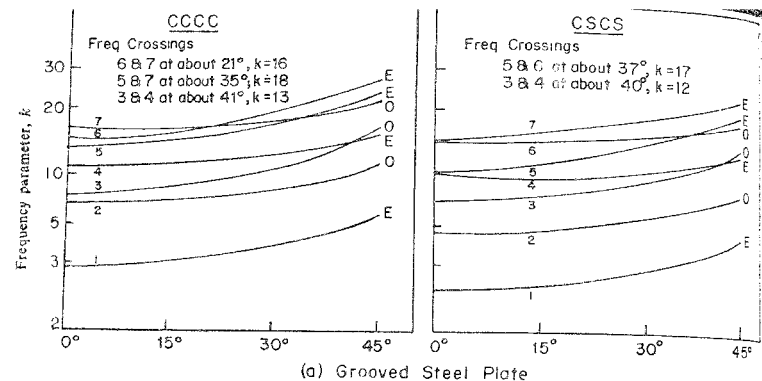


FIG. 2
 Variation of Frequencies with Skew Angle

Fundamental: $k=8.166$

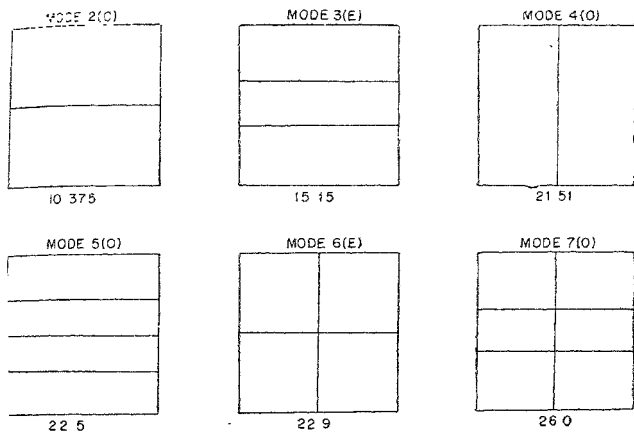


FIG. 3

Nodal Patterns of Rhombic Plate (CCCC), $\psi=0^\circ$ (Boron-Epoxy)

Fundamental: $k=8.807$

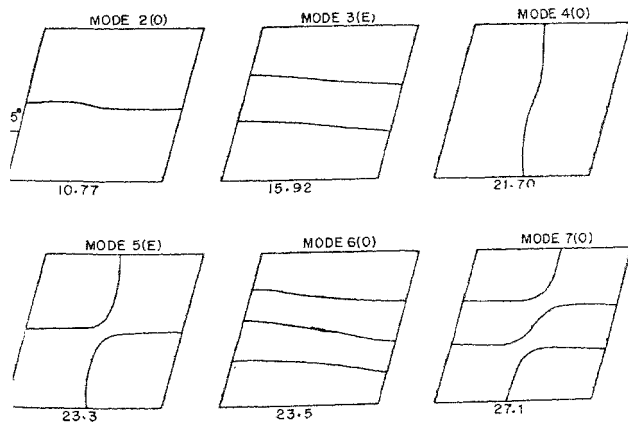


FIG. 4

Nodal Patterns of Rhombic Plate (CCCC), $\psi=15^\circ$ (Boron-Epoxy)

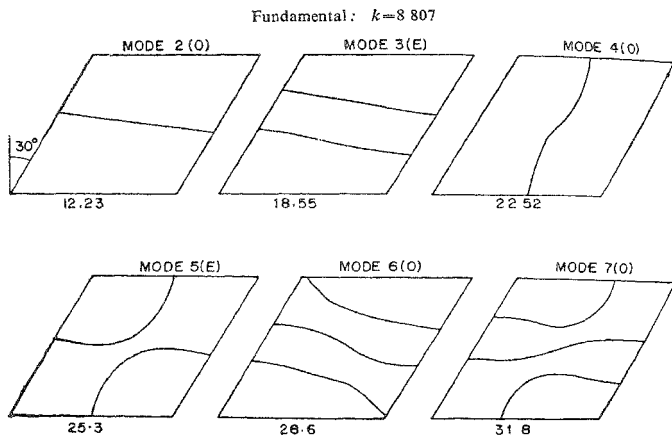


FIG. 5
Nodal Patterns of Rhombic Plate (CCCC), $\psi=30^\circ$ (Boron-Epoxy)

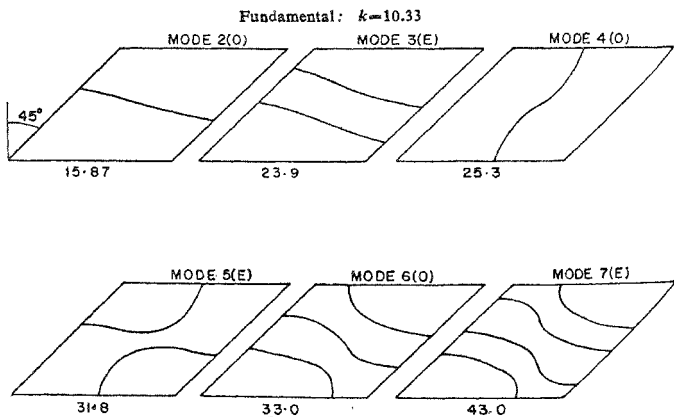


FIG. 6
Nodal Patterns of Rhombic Plate (CCCC), $\psi=45^\circ$ (Boron-Epoxy)

Fundamental: $k=7.879$

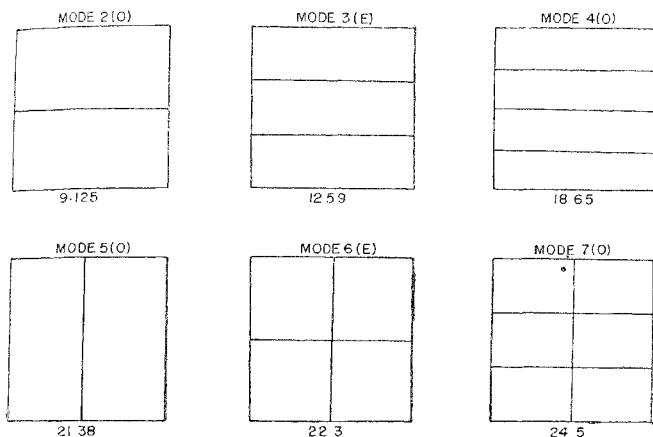


FIG. 7

Nodal Patterns of Rhombic Plate (CSCS), $\psi=0^\circ$ (Boron-Epoxy)

Fundamental: $k=7.966$

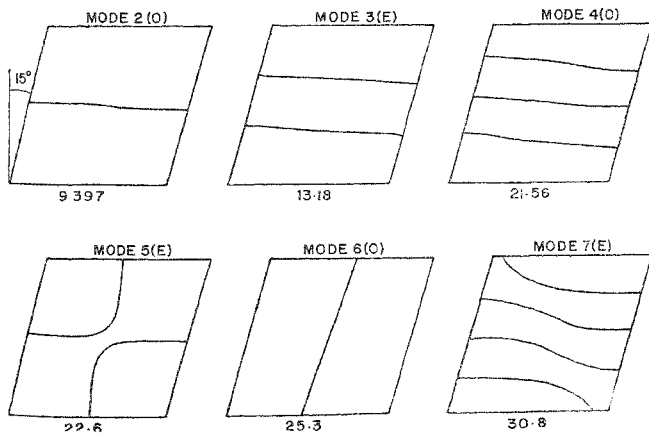


FIG. 8

Nodal Patterns of Rhombic Plate (CSCS), $\psi=15^\circ$ (Boron-Epoxy)

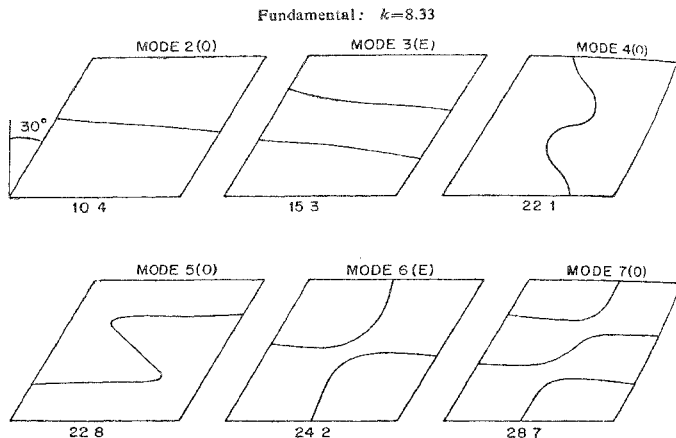


FIG. 9

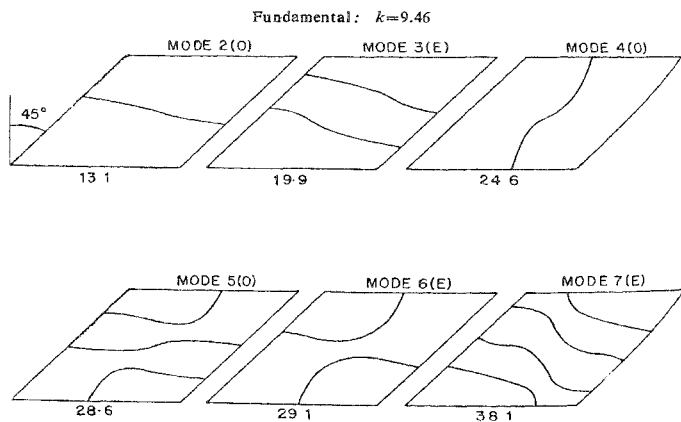
Nodal Patterns of Rhombic Plate (CSCS), $\psi=30^\circ$ (Boron-Epoxy)

FIG. 10

Nodal Patterns of Rhombic Plate (CSCS), $\psi=45^\circ$ (Boron-Epoxy)

From the results given in Tables 4, and 5 and 6, it could be seen that the buckling coefficients vary widely with the orthotropic property of the plate, increasing in magnitude with the rigidity constant α ($=D_{x1}/D_{y1}$). It is also seen that the buckling coefficients under direct compression N_x , vary only very slightly with skew angle in the case of boron-epoxy which is highly anisotropic in comparison with fibre glass-epoxy and grooved steel plate. It is useful to compare this feature with the corresponding range of variation in the case of isotropic plate. This comparison shows that the range of variation in the latter case is more. From this it appears that, on the whole, the more highly unidirectional the orthotropic properties are, the less effective is the influence of skew angle in raising the magnitude of the buckling coefficient. In the case of shear, two critical values exist, positive and negative, positive shear (acting in a way so as to reduce the skew angle) being always less than the negative shear for the combinations of boundary condition and material properties considered. While the positive shear decreases with the skew angle, the negative shear increases in magnitude with the increase in the skew angle as observed in the case of isotropic plates.

5. CONCLUSIONS

The vibration and buckling problems of orthotropic skew plates with different combinations of edge conditions are formulated in a unified manner using the variational method of Ritz. Numerical results are obtained for two sets of edge conditions and three sets of orthotropic properties. Crossing of frequency curves is seen to take place as in the case of isotropic plate. The effect of orthotropy on the nodal patterns and their symmetries is studied. The buckling coefficients are obtained under compression (N_x) and shear (N_{xy}) for these configurations. For buckling under shear (oblique components), two critical values exist, with the magnitude of positive shear being less as in the case of isotropic plate.

ACKNOWLEDGEMENT

We express our thanks to Mr. Mahabaliraja for his extensive help in the computational work involved.

TABLE 4

Buckling Coefficients \bar{P}_x and \bar{R}_{xy} for a Clamped Rhombic Plate
Material: Steel Plate Grooved on one side $\alpha=1.265$; $\gamma=0.28$; $\delta=0.339$

Boundary conditions and loading	Skew Angle	M	N	Matrix size	Buckling coefficients \bar{R}_x and \bar{R}_{xy}
CCCC N_x alone	0°	6	6	18	11.1 (E)
	15°	6	6	18	11.5 (E)
	30°	6	6	18	13.0 (E)
	45°	8	8	32	15.8 (E)
CCCC N_{xy} alone	0°	6	6	18	± 15.8 (E)
	15°	6	6	18	12.1 (E) -23.3 (E)
	30°	6	6	18	10.6 (E) -40.6 (E)
	45°	8	8	32	10.4 (E) -89.4 (E)
CSCS N_x alone	0°	6	6	18	7.72 (E)
	15°	6	6	18	8.11 (E)
	30°	6	6	18	9.49 (E)
	45°	8	8	32	12.4 (E)
CSCS N_{xy} alone	0°	6	6	18	± 13.9 (E)
	15°	6	6	18	10.8 (E) -20.4 (E)
	30°	6	6	18	9.45 (E) -35.7 (E)
	45°	8	8	32	9.39 (E) -78.7 (E)

TABLE 5

Buckling coefficients \bar{R}_x and \bar{R}_{xy} for CCCC and CSCS Rhombic Plates
 Material: Fibre glass-epoxy $\alpha=2,963$. $\gamma=0.25$, $\delta=0.450$

Boundary conditions and Loading	Skew Angle	M	N	Matrix size	Buckling coefficients \bar{R}_x and \bar{R}_{xy}
CCCC N_x alone	0°	6	6	18	18.5 (E)
	15°	6	6	18	19.0 (E)
	30°	6	6	18	20.9 (E)
	45°	8	8	32	25.0 (E)
CCCC N_{xy} alone	0°	6	6	18	± 24.5 (E)
	15°	6	6	18	20.1 (E) -32.7 (E)
	30°	6	6	18	17.8 (E) -50.8 (E)
	45°	8	8	32	17.1 (E) -100 (E)
CSCS N_x alone	0°	6	6	18	14.9 (E)
	15°	6	6	18	15.3 (E)
	30°	6	6	18	16.8 (E)
	45°	8	8	32	20.4 (E)
CSCS N_{xy} alone	0°	6	6	18	...
	15°	6	6	18	18.7 (O) -30.8 (E)
	30°	6	6	18	16.6 (O) -46.9 (E)
	45°	8	8	32	15.9 (O) -90.9 (E)

TABLE 6

Buckling coefficients \bar{R}_x and \bar{R}_y for CCCC and CSCS Rhombic Plates
 Material: Boron-epoxy $\alpha=11.48$, $\gamma=0.28$, $\delta=0.276$

Boundary conditions and loading	Skew angle	M	N	Matrix size	Buckling coefficients \bar{R}_x and \bar{R}_y
CCCC N_x alone	0°	6	6	18	51.8 (E)
	15°	6	6	18	51.5 (E)
	30°	6	6	18	51.4 (E)
	45°	8	8	32	54.4 (E)
CCCC N_{xy} alone	0°	6	6	18	± 49.7 (0)
	15°	6	6	18	44.2 (0) -59.4 (0)
	30°	6	6	18	40.9 (0) -79.0 (E)
	45°	8	8	32	39.6 (0) -123 (E)
CCCC N_x alone	0°	6	6	18	48.4 (E)
	15°	6	6	18	47.7 (E)
	30°	6	6	18	46.4 (E)
	45°	8	8	32	47.0 (E)
CCCC N_{xy} alone	0°	6	6	18	± 47.9 (0)
	15°	6	6	18	42.8 (0) -56.2 (0)
	30°	6	6	18	39.2 (0) -73.4 (0)
	45°	8	8	32	36.8 (0) -117.1 (E)

REFERENCES

1. George Lubin (Ed.), Handbook of Fibreglass and Advanced Plastics, Polymer Technology Series, 1969.
2. Brontman, L. J. and Krock, R. H. (Eds.), Modern Composite Materials, Addison Wesley, 1967.
3. Calcote, L. R. The Analysis of Laminated Composite Structures, Van Nostrand Reinhold Company, 1969.
4. Hearmon, R. F. S. *J. Appl. Mech.*, 1959, 26, (3-4), 537.
5. Huffington, Jr. N. H. and Hoppman. *Ibid*, 1958, 25, (3), 389.
6. Hearmon, R. F. S. *Ibid*, 1959, 26, (2), 307.
7. Kanazawa, T. and Kawai, T. *Proceedings of the Second Japan National Congress on Appl. Mechs*, 1952, 333.
8. Bert, W. C. and Mayberry, L. B. *J. of Composite Materials*, 1969, 3, 252.
9. Ashton, J. E. and Anderson, J. D. *General Dynamics Research and Engg*, Report, 1968, FZM-5008.
10. Timoshenko. S. P. and Gere, J. M. *Theory of Elastic Stability*, Mc.Graw-Hill Book Company Inc., 1961.
11. Lekhnitskii, S. G. *Anisotropic Plates*, Gordon and Breach Science Publishers, 1968.
12. Das, Y. C. *Applied Scientific Research*, 1963. 2 (A), 97.
13. Holston, A., *AIAA J.* 1970, 8, (7), 1352.
14. Wittrick, W. H., *The Aeronautical, Quarterly*, 1952, 4, 83.
15. Shuleshko, P., *Ibid*, 1957, 8, 145.
16. Lurie, H. *J. of Aeronautical Sciences*, 1951, 18, 139.
17. Durvasula, S. and Srinivasan, S. *J. of Aeronautical Society of India*, 1967, 19 (3), 65.
18. Chamis, C. C. *Proceedings of the American Society of Civil Engineers*, 1969, 2119
19. Fraser, H. R. and Miller, E. R. *AIAA J.* 1970, 8, (4) 707.
20. Ashton, J. E. and Love, T. S. *General Dynamics Research and Engineering Report*, 1968, FZM-4992.
21. Ashton, J. E. *Ibid*, 1967, FZM, 4899.
22. Nair, P. S. and Durvasula, S. *Report No. AE 264-S, Department of Aeronautical Engineering, Ind. Inst. of Sci., Bangalore-1970.*
23. ————— *Report No. AE 267 S, Department of Aeronautical Engineering, Ind. Inst. of Sci., Bangalore, 1970.*
24. Prabhu, M. S. S. and Durvasula, S. *Report No. AE 266 S, Department of Aeronautical Engineering, Ind. Inst. of Sci., Bangalore, 1970.*
25. Felgar, R. P. *University of Texas Bureau of Engineering Res., Circular No. 14, 1950.*
26. Durvasula, S., Bhatia, P. and Nair, P. S *Report No. AE 220, S. Department of Aeronautical Engineering, Ind. Inst. of Sci., Bangalore, 1969.*
27. Durvasula S. *Report No. AE 219 S, Department of Aeronautical Engineering, Ind. Inst. of Sci., Bangalore, 1970.*